Surface Science 156 (1985) 548–555
North-Holland, Amsterdam

EFFECTS OF THREE-BODY INTERACTIONS ON THE STRUCTURE OF CLUSTERS

Estela BLAISTEN-BAROJAS * and Hans C. ANDERSEN

Department of Chemistry, Stanford University, Stanford, California 94305, USA

Received 10 July 1984

The structure of 54 and 147 atom clusters was studied using molecular dynamics at constant temperature and incorporating three-body interactions to the usual pairwise additive potentials among atoms. The effects of three-body interactions of the triple-dipole and exchange overlap type on the aggregation of clusters are: (1) to diminish the coordination number resulting in a global expansion of the clusters; (2) to increase internal disorder in such a way as to lower the crystallization temperature; (3) to favor certain features characteristic of random close packing of spheres at the expenses of destroying locally paired tetrahedra and octahedra, in the temperature range $0.25 \leqslant T \leqslant 0.4$.

1. Introduction

In the last decade, structural phenomena in small systems such as drops and dense aggregates of atoms have deserved various degrees of attention. Two kinds of computer simulation have been used in this direction, the atomistic building up of clusters [1,2] and the Monte Carlo or molecular dynamics methods [3]. The first group of works is based on various static criteria for packing atomic clusters. The second group of works were focused on problems such as: the local density of small systems [4–6], vaporization [5], the local potential energy [7,8], the structure of a microcrystal in the process of a phase transition [9], the free energy and surface energy [9,10] dependence on the number of atoms, the structure and interference functions [8,11] among others.

On the other hand, much effort is paid in the aggregation of molecules to n-body effects. These contributions to the energy, although small, do play an important role on the theoretical determination of the best molecular geometry [12]. We are interested in this work to analyze the importance of three-body interactions versus pairwise additive interactions in what concerns the structure of atomic clusters.

* Permanent address: Instituto de Fisica, Universidad Nacional Autónoma de México, Apartado Postal 20-364, 01000 México, DF, Mexico.

0039-6028/85/$03.30

Our purpose is first to review some of the previous cooling experiments with the use of molecular dynamics at constant temperature [13] for clusters of atoms interacting via pair potentials. In addition we will incorporate to the dynamics the non-pair-additive forces resulting from a model three-body potential, V_3, for every triplet of atoms in the cluster. At least partly because of limited information in the literature, V_3 has frequently been approximated by the triple-dipole energy of Axilrod, Teller [14] and Muto [15]. However, more extensive information on V_3 is available at present and models based on Hartree–Fock [16] and dispersion energy results [14] have been constructed for weakly bound trimers [17,18].

The organization of the paper is as follows. In section 2 we define the cluster, describe the methods used, and discuss a phase transition for the two-body system. In section 3, we give the results of adding the three-body potential to the dynamics, present a novel approach to interpret the profile of the radial distribution function $g(r)$ and conclude with a brief discussion.

2. Model and methods

Let us define a cluster as that aggregate of N atoms held together by the intermolecular forces themselves. The range of interaction between atoms has a finite cutoff radius, r_c, mainly because of computational requirements. We keep a configuration of atoms as permitted if the atoms on the cluster surface are at distances from their nearest neighbors smaller than r_c. Whenever the energy of an atom is large enough to push it outside the cutoff, we stop the simulation. This last condition restricts us to study clusters at low temperatures and presumably only in the solid phase.

Let the coordinates of the N atoms be $\boldsymbol{r}_1, \boldsymbol{r}_2, \ldots, \boldsymbol{r}_N$ and the cluster Hamiltonian be

$$H(\boldsymbol{r}^N, \boldsymbol{p}^N) = \sum_{i=1}^{N} p_i^2/2m + \sum_{i<j}^{N} V_2(r_{ij}) + \sum_{i<j<k}^{N} V_3(r_{ij}, r_{ik}, r_{jk}), \tag{1}$$

where $r_{ij} = |\boldsymbol{r}_i - \boldsymbol{r}_j|$ and $\boldsymbol{r}_i$, $\boldsymbol{p}_i$ are conjugated variables.

The pair interaction V_2 is a truncated Lennard-Jones potential equal to zero at a cutoff distance d_2:

$$V_2(r) = \begin{cases} 4\epsilon\left\{\left[(\sigma/r)^{12} - (\sigma/r)^6\right] - \left[(\sigma/d_2)^{12} - (\sigma/d_2)^6\right]\right\}, & r < d_2; \\ 0, & \text{otherwise.} \end{cases} \tag{2}$$

The three-body potential V_3 is a function [16,17] that fits well the quantum-

mechanical data for rare gases and beryllium atoms,

$$V_3(r, s, t) = \left\{ -A \exp[-\alpha(r+s+t)] + Z/(rst)^3 \right\}(1 + 3\cos\theta_r \cos\theta_s \cos\theta_t), \tag{3}$$

where r, s, t are the sides and θ_r, θ_s, θ_t the three angles of the triangle formed by a triplet of atoms. The first term on the RHS stands for the exchange overlap contribution of intensity A and range measured by α. This contribution is short range, and so it modifies the repulsion introduced by the pair potential. The second term is a dispersion energy result [14] of intensity obtained from third-order perturbation theory. For the calculations, the three-body potential V_3 goes to zero at a cutoff distance d_3, much in the same way as V_2.

The density of the cluster is defined as $\rho = N_c/\Omega_c$, where N_c denotes the number of atoms contained in a sphere of radius $R_c = \Sigma_i |\boldsymbol{r}_i - \boldsymbol{r}_{cm}|/N$, $\boldsymbol{r}_{cm}$ being the cluster center-of-mass radius vector and Ω_c is the volume of a sphere with radius R_c. This definition gives an idea of which is the density at the cluster "core". Atoms outside the core make up the cluster "surface".

$\tau = (m\bar{u}^2/\epsilon)^{1/2}$.

Andersen introduced the constant-temperature molecular dynamics and we refer to his work [13] for details. The main ingredient for this dynamics is that the time average of a mechanical state $f(\boldsymbol{r}^N, \boldsymbol{P}^N)$ of the system is equal to the canonical ensemble average of that function. For computational purposes we adopt reduced units: $r^* = r/\sigma$, $\rho^* = \rho\sigma^3$, $T^* = k_B T/\epsilon$, $V^* = V/\epsilon$, $t^* = t/\tau$, $\tau = (m\sigma^2/\epsilon)^{1/2}$. The equations of motion were solved using a time step of 0.01τ in all cases, and the atoms were initially arranged as those in a sphere cut from a well-equilibrated configuration of the bulk liquid phase at high temperatures [19]. Typically, runs lasted 120τ for systems with bare two-body interactions and between 30 and 60τ when three-body interactions were added.

We described now one computer experiment for the 147 cluster with only two-body interactions among the atoms of the system. Brian and Burton [9] reported a phase transition from solid to liquid in a 100 atom cluster at $T^* = 0.31$ to 0.33. They detected the transition only when the cluster was prepared by heating slowly from a lower energy. In order to locate such transition, and in view of our constant-temperature dynamics, we proceed as follows. First, let us start from an initial configuration chosen as explained at the end of the previous paragraph. Secondly, let us cool at a very slow rate of $\Delta T^*/\Delta t^* = 8.3 \times 10^{-5}\ \tau^{-1}$ and sweep the region $0.25 \leqslant T^* \leqslant 0.38$. In fig. 1a we plot the average potential energy per atom as a function of temperature. The curve has definitely two slopes at $T^* = 0.29$–0.3, which is a somehow lower temperature than Brian and Burton's T_c. We can say that we are seeing a diffusionless transition from an amorphous with ingredients of random close packing phase [20] to a quasi-fcc phase.

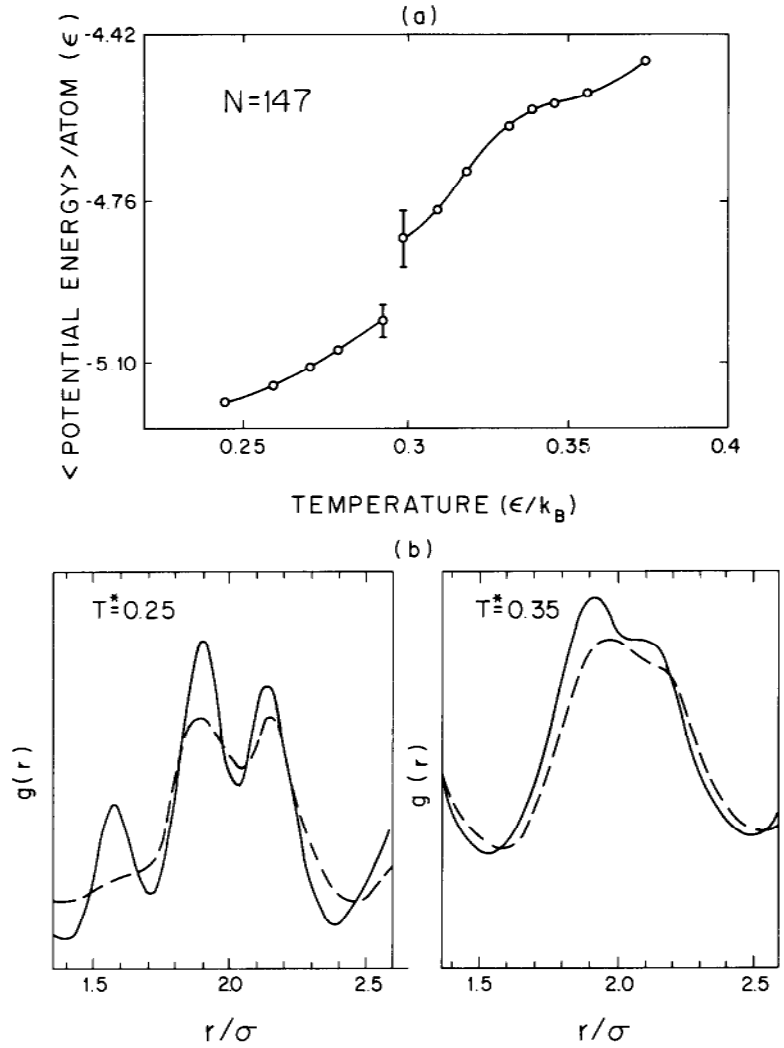

Fig. 1. (a) Average potential energy per atom as a function of temperature for 147 atom cluster. Typical error bars are shown. (b) Radial distribution function second peak for two different temperatures: Full lines correspond to the bare two-body calculation and dashed lines are the result when three-body interactions are added ($Z^* = 0.15$, $\alpha^* = 4.5$, $A^* = 2\times10^4$). The vertical scales are different.

The above statement is based on an analysis of the radial distribution function. In fig. 1b we show $g(r)$ in the region of second-neighbor distances for two temperatures, before and after the transition. The function's first maximun is at $r_0^* = 1.09$. At $T^* = 0.35$, $g(r)$ presents a splitted second peak at $r^* \approx 3^{1/2} r_0^*$. At $T^* = 0.25$, the radial distribution function has an extra and

well-defined maximum at $r = 2^{1/2} r_0^*$. This last peak is characteristic of the fcc crystal, although the ratios between $g(r)$ values at the maxima are not those of a perfect crystal.

To study these discrepancies we propose a classification of the distances composing $g(r)$ in the following way [19]. Let us classify the second-neighbor distances between atoms A and B as belonging to "geometrical arrangements"

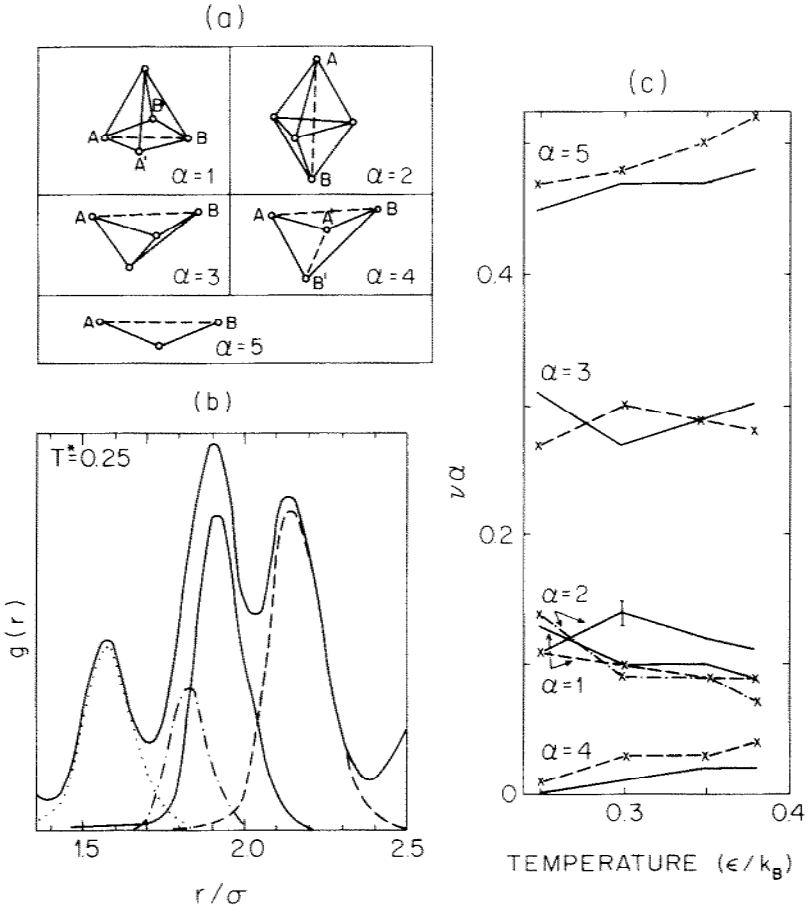

Fig. 2. (a) The five geometrical arrays with second-neighbor distrancese (dotted lines). Full lines join nearest-neighbor atoms. (b) Decomposition of the radial distribution function shown in fig. 1b for the bare two-body 147 atom cluster. The lower curves indicate the contribution to the five structures shown in fig. 2a: $\alpha = 1$ (...), $\alpha = 2$ (– · –), $\alpha = 3$ (———), $\alpha = 5$ (— — —). The array $\alpha = 4$ gives a contribution not seen in the scale. (c) Correlation coefficients as a function of temperature. Full lines correspond to the two-body calculation and dotted lines are the result when three-body interactions are added ($Z^* = 0.15$, $\alpha^* = 4.5$, $A^* = 2 \times 10^4$). A typical error bar is shown.

formed by A and B and by at most three common nearest neighbors. Only five structures containing second-neighbor distances are obtained using this procedure (fig. 2a): (1) half octahedra (HO); (2) double tetrahedra sharing one face (DT); (3) double equilateral triangles with one common side (DET); (4) double isosceles triangles sharing the unequal side; and (5) linear arrays of 3 atoms with 2 nearest-neighbor distances. Interestingly enough, these five smallest geometrical arrangements are the only structures into which all second-neighbor distances can be distributed. Therefore, we can decompose the distances into partial contributions to $g(r)$:

$$g(r) = \sum_{\alpha=1}^{5} g_\alpha(r), \quad 1.35 \leqslant r^* \leqslant 2.3 \tag{4}$$

as is pictured in fig. 2b, for $T^* = 0.25$. At lower temperatures we have larger occurrence of half and full octahedra at second-neighbor distances $2^{1/2} r_0^*$ which is an indication that an fcc quasicrystalline phase is favored. At $T^* = 0.3$ and higher temperatures, many more "twinned" tetrahedra (DT) are formed, possibly indicating the presence of incomplete icosahedra or hexagonal close packed regions. Thus, there is indication that a conformational transition is taking place in this range of temperature.

3. The three-body effects

One important influence is that the ratio between the averages of the V_3 to the V_2 terms in the potential energy $\langle V_3 \rangle / \langle V_2 \rangle$, is a function of the number of atoms in the cluster, decreases with temperature, and is a negative quantity. This fact makes it difficult to propose a criterion for scaling the three-body effects into effective two-body parameters.

The first peak of the radial distribution function $g(r)$ as a function of V_3 parameters [19] is shifted towards larger distances when Z is increased. The exchange overlap term A opposes this effect, although slightly. The overall effect is an expansion of 1% in the nearest-neighbor distances between the cluster atoms and consequently a reduction of 5–10% in the coordination number (in the range $0.25 \leqslant T^* \leqslant 0.42$ and for finite number of atoms).

A more interesting effect of V_3 is how it affects the structure of the radial distribution function in the range of the second-neighbor distances. In fig. 1b we show the smoothing of $g(r)$ maxima due to three-body effects when compared to the calculation with bare two-body interactions. It is in this range of distances where the outcome of favored triplets of atoms, other than equilateral triangles, can be conveniently discussed in terms of the $g_\alpha(r)$ from eq. (4). Let us define a frequency of occurrence for each of the five geometrical arrays of atoms of fig. 2a: $\nu_\alpha = n_\alpha / n_T$, where $n_T = \Sigma n_\alpha$ and $\alpha = 1$ to 5. In fig.

2a we have represented the ν_α as functions of temperature. Changes in the packing, as we can infer from this picture, are not drastic. However, between $T^* = 0.25$ and $T^* = 0.3$ the two-body system is suffering a structural change. At lower temperatures, when the ratio of three- to two-body energies is larger, we find that DTs ($\alpha = 2$) are favored at the expenses of DETs ($\alpha = 3$). When temperature is raised in the system ($T^* > 0.3$) the ratio three- to two-body energies diminishes, and yet the α are almost constant except for an increase of the linear arrays ($\alpha = 5$). A model of disorder is a random close packing of spheres [20] where only ν_3 and ν_5 are present. Temperature enhances such situation. Summarizing, three-body interactions produce disorder, as if an extra source of temperature would be plugged to the cluster. As a function of temperature, three-body interactions produce the destruction of all geometrical structures with a tendency to favor more the linear ($\alpha = 5$) and the planar ($\alpha = 4$) arrays as well as triplets with sides larger than 2.3.

Another analysis can be performed to break $g(r)$ into partial functions associated to the core, surface, and intermediate regions in the cluster. Except for the distances within the core being shorter then those in the core–surface and in the surface regions, the distribution of geometrical arrays in the three regions are very much like those previously discussed for the whole cluster. The surface contains the largest proportion of arrays $\alpha = 4$ and triplets with at least two sides larger than 2.3.

A search for the mutual arrangement of DTs shows that pairs of DTs prefer to share only one atom in clusters with and without three-body terms [19]. Clusters with bare two-body interactions have a significant increase of paired DTs sharing 4 atoms (incomplete five-fold symmetry motifs) at $T^* = 0.3$. This is not so for systems with three-body terms. We can interpret this effect by saying that locally interconnected icosahedra are suffering a conformational rearrangement at T_c only for the bare two-body systems.

We have demonstrated that for finite systems and when the exchange overlap term is small, the effect of three-body interactions is to increase slightly the nearest-neighbor distances and decrease the coordination number. We have also shown that three-body interactions favor the less crystalline packing and no temperature activated transition seems to appear (at least in the range $0.25 \leqslant T^* \leqslant 0.38$). In the range of temperatures of this study, there is little evidence of a large number of icosahedral motifs for the 147 cluster with two- and three-body potentials. Finally, let us say that the analysis of the radial distribution function second peak might be interesting for the study of amorphous phases of metals and alloys. Further work is now in process to search for effects of the non-pair-additive model on the cluster surface tension [21] changes during a slow cooling or slow heating experiment.

Acknowledgements

E.B.B. acknowledges the Fulbright and AAUW Foundations for financial support given through a research fellowship and the CONACyT (México) for partial support.

References

[1] J.A. Barker and M.R. Hoare, Nature 257 (1975) 120.
[2] M.R. Hoare, Advan. Chem. Phys. 40 (1979) 49.
[3] F.F. Abraham, IBM Research Report RJ 3522 (41579) (1982).
[4] J.K. Lee, J.A. Lee, J.A. Barker and F.F. Abraham, J. Chem. Phys. 58 (1973) 3166.
[5] F.F. Abraham, J.K. Lee and J.A. Barker, J. Chem. Phys. 60 (1974) 246.
[6] A.C.L. Öpitz, Phys. Letters 47A (1974) 439.
[7] D.J. McGinty, J. Chem. Phys. 58 (1973) 4733.
[8] J. Farges, M.F. Feraudy, B. Raoult and G. Torchet, J. Physique 38 (1977) C2-47.
[9] C.L. Brian and J.J. Burton, J. Chem. Phys. 63 (1975) 2045.
[10] E.N. Brodskaya and A.I. Rusanov, Kolloid. Zh. 39 (1977) 636, 646.
[11] J. Farges, M.F. Feraudy, B. Raoult and G. Torchet, Surface Sci. 106 (1981) 95.
[12] O. Novaro, Kinam 2 (1980) 175.
[13] H.C. Andersen, J. Chem. Phys. 72 (1980) 2384.
[14] B.M. Axilrod and E. Teller, J. Chem. Phys. 11 (1943) 299.
[15] Y. Muto, Proc. Phys. Math. Soc. Japan 17 (1943) 629.
[16] L.W. Bruch, O. Novaro and A. Flores, J. Chem. Phys. 67 (1977) 2371.
[17] L.W. Bruch, E. Blaisten-Barojas and O. Novaro, J. Chem. Phys. 67 (1977) 4701.
[18] E. Blaisten-Barojas, O. Novaro and L.W. Bruch, Mol. Phys. 37 (1979) 599.
[19] E. Blaisten-Barojas, Kinam 6A (1984) 71.
[20] J.M. Ziman, Models of Disorder (Cambridge Univ. Press, London, 1979) p. 78.
[21] A.L. Benavides, H.T. Davis, M.I. Guerrero and E. Martina, Kinam 5 (1983) 285.